A Three-Barrier Model for the Hemocyanin Channel

XIMENA CECCHI, OSVALDO ALVAREZ, and RAMON LATORRE

From the Department of Biology, University of Chile, Santiago, Chile, and the Department of Physiology, Harvard Medical School, Boston, Massachusetts 02115

ABSTRACT Keyhole limpet hemocyanin forms ion-conducting channels in planar lipid bilayer membranes. Ionic current through the open hemocyanin channel presents the following characteristics: (*a*) it is carried mainly by cations; (*b*) it is a nonlinear function of membrane potential; (*c*) channel conductance is a saturating function of ion activity; (*d*) it shows ionic competition. A model for the open hemocyanin channel is developed from absolute reaction rate theory. The model calls for three energy barriers in the channel. Two energy barriers represent the entrance and exit of the ion into and out of the channel. The third barrier separates two energy minima that represent two binding sites. Furthermore, only one ion is allowed inside the channel at a given time. This model is able to recreate all the hemocyanin channel characteristics found experimentally in negatively charged and neutral membranes.

INTRODUCTION

Keyhole limpet hemocyanin (KLH) is able to interact with planar lipid bilayer membranes and form voltage-dependent channels (Alvarez et al., 1975; Latorre et al., 1975). Latorre et al. (1975) showed that the voltage dependence of the conductance of many-channeled membranes arises from both the voltage-dependent distribution among several discrete conductance steps and the voltage dependence of the conductance states themselves.

Hemocyanins are the oxygen-transporting blood proteins that occur freely dissolved in the blood of many invertebrates (van Bruggen et al., 1962 *a* and *b*; 1963). At neutral pH and in dilute salt solutions, hemocyanins are roughly cylindrical in shape (van Bruggen et al., 1963; Fernandez-Moran et al., 1966; Mellema and Klug, 1972). In particular, electron microscopy studies indicate that KLH, with a molecular weight of $\sim 10^7$, is a cylinder in which both height and length are ~30 nm (McIntosh et al., 1980). Recently, McIntosh et al. (1980) examined the interaction of KLH with lipid monolayers, lipid vesicles, and planar lipid bilayers. They found that KLH produces a characteristic 7-nm-diameter, ring-shaped particle associated with the bilayer. Furthermore, the center of the ring accumulates stain, and the diameter of the stain in the center is ~2 nm. This central pool of stain may be related to the conducting channel, but its diameter cannot be equated with the actual diameter of the channel. It is noteworthy that from the several hemocyanins tested by Mc-

Intosh et al., the only one capable of producing the 7-nm ring and increasing the conductance of lipid bilayer membranes was KLH. It is likely, therefore, that these structures seen in monolayers and lipid bilayer systems, and not the whole hemocyanin molecule, are responsible for channel formation in planar lipid bilayer membranes. Another important feature of the structure found by McIntosh et al. in monolayers and lipid vesicles is that the particle associated with the membrane projects into the aqueous phase by 25–45 Å. If the central pool of stain seen in the structure can be identified with the mouth of the channel, ion transport through the hemocyanin channel starts away from the bilayer surface.

There is compelling evidence that the ion permeabilities of biological membranes are localized in special structures called pores or channels (Hille, 1970; Ehrenstein and Lecar, 1972). It has become clear in the past few years that ion permeation through sodium and potassium channels in nerve and muscle cannot be completely described with continuum electrodiffusion theory. To explain such a variety of phenomena as ion competition, saturation, and the nonlinear instantaneous current-voltage relationships found in biological membranes, channels can be represented by a sequence of "binding sites" separated by activation energy barriers. In the potential energy profile, these sites are energy minima (Woodbury, 1971; Hille, 1975; Hille and Schwarz, 1978). These types of models are based on chemical rate theory (Glasstone et al., 1941; Parlin and Eyring, 1954).

In this paper, we present the characterization of the ion transport through the hemocyanin channel. We develop here a three-barrier model of the channel that accounts for the saturation of the channel conductance with ion concentration, ion competition, and nonlinear current-voltage relationships found for the open hemocyanin channel. Furthermore, we found that the single-channel conductance measured at low voltages is the same in the negatively charged soybean lipid membranes and in neutral phosphatidylethanolamine membranes. We explain this property on the basis of the unique structural features of the hemocyanin channel, i.e., the ion entrance to the channel is located >1 Debye length from the bilayer surface. A preliminary account of this work has been given (Alvarez et al., 1977).

METHODS

Membranes were formed by apposition of two monolayers as described by Montal and Mueller (1972). In most of the experiments, monolayers were formed by placing 10 μl of a mixture of asolectin and cholesterol dissolved in 95% hexane and 5% decane. Total lipid concentration was 25 mg/ml, and the cholesterol mole fraction was 0.5. Asolectin is phosphatidylcholine type II-S obtained from soybean. It is a mixture of many lipids containing ~20% negatively charged phospholipids. Cholesterol was Sigma grade standard for chromatography. Both asolectin and cholesterol are from Sigma Chemical Co. (St. Louis, Mo.), and all organic solvents were obtained from Eastman Kodak Co. (Rochester, N. Y.). In some experiments, membranes were formed using bacterial phosphatidylethanolamine (Supelco, Inc., Bellefonte, Pa.), which was dissolved to 12.5 mg/ml in 95% hexane plus 5% decane.

Aqueous subphase was buffered to pH 7 using 5 mM Tris-chloride (Trizma; Sigma

Chemical Co.). Hemocyanin, lyophilized powder, from keyhole limpet (Calbiochem-Behring Corp., San Diego, Calif.) was dissolved in 5 mM Tris buffer, pH 8.5, to 10 mg/ml. Hemocyanin solution was added to one side of the membrane only. This side will be called *cis*, and the other side will be called *trans*.

Electrical Measurements

The hemocyanin-containing side of the membrane, the *cis* side, was connected to a current-voltage converter through an Ag/AgCl electrode. The *trans* side was connected to a function generator using another Ag/AgCl electrode. Therefore, the *cis* side was virtual ground, and the potential was applied to the *trans* side. A positive current, driven by a positive voltage, is defined as cation flow into the *cis* side.

Single-Channel Conductance

For single-channel conductance measurements, a high-input resistance, low-input bias current amplifier was built using field effect transistors (type AD-830; Analog Devices, Inc., Norwood, Mass.). To improve signal-to-noise ratio, the current was sampled once every cycle of the power line. Sampling circuit was activated by an oscillator triggered by the line alternating current. The circuit effectively rejects power line current pick up without damping the signal.

Single-channel conductance was measured from the discrete current steps obtained at −50 mV as hemocyanin is incorporated into the membrane. The average current before and after the current step was calculated using 5–100 data points. Channel conductance was calculated from the difference of these two values.

Instantaneous Current-Voltage Curves

Current-voltage curves are obtained by measuring the current during brief voltage pulses of various amplitudes. Voltage pulses were given with an interval of 200 ms and lasted 1.5 ms. One current sample was taken 1 ms after the onset of the pulse. One *I-V* curve consists of 250 data points taken with an interval of 2 mV, spanning the range from −250 to +250 mV. Voltage pulses were generated using a 12-bit digital to analog converter (DAC-DG12B; Datel, Canton, Mass.) under computer control. The transient current resulting from the charge of membrane capacitance was subtracted using a differential ammeter (Alvarez and Latorre, 1978). One input of the ammeter was connected to the membrane and the other was connected to a capacitor and a series resistance simulating the membrane. Digitized *I-V* curves were stored in a magnetic diskette for later curve-fitting analysis. To compare the theoretical current-voltage relationships with those obtained experimentally, the experimental *I-V* curves were scaled down using the single-channel conductance obtained at −50 mV. This procedure is validated by the direct comparison of single-channel and multi-channel *I-V* curves, which demonstrate that all channels are inserted into the bilayer in the same way (Alvarez et al., 1975). In addition, we have followed the insertion of ~50 channels into the bilayer. We found that all channels had the same orientation with respect to the electric field. This sets an upper limit of 2% of channels oriented in the wrong way.

Fast-Current Measurements

Current time-course after a voltage jump was measured using a differential ammeter with a rise time of 1 μs (Alvarez and Latorre, 1978). To compensate for capacitative current surge, the voltage pulse was given simultaneously to the membrane and to a resistance-capacitor combination. Voltage pulses were given with a pulse generator

built in our laboratory with a settling time of 250 ns. Currents passing through the membrane and resistance-capacitance (R-C) circuit were adjusted so as to get the best rejection of the capacitative surge current. Hemocyanin was added to the *cis* side of the membrane and the solution was stirred using magnetic bars.

To measure the current time-course, positive and negative voltage pulses were used. One experiment consists of 128 pairs of pulses with the same amplitude but alternating polarity. Current was digitized by a fast, six-bit analog to digital converter (610-B; Biomation, Cupertino, Calif.). The first record was stored in digital memory (a matrix of 256 locations of 16 bits) and each succeeding record was added to the previous contents of the digital memory. At the end of the experiments, the memory matrix contains the point-by-point difference of the positive and negative currents. This procedure was carefully checked using resistors and capacitors in the place of the membrane. In these conditions, no residual current was observed.

Zero-Current Potentials

Membranes were formed under 5 mM Tris-Cl buffer and hemocyanin was added to one side (*cis*). Potassium sulfate was added to the *cis* side to a final concentration of 14 mM. Lithium or potassium sulfate was added to the *trans* side to reach various final concentrations. Both solutions were constantly stirred. Potential was measured through Ag/AgCl electrodes connected to a high-impedance voltage follower made using low-gate current field effect transistors (AD-830; Analog Devices, Inc.). In some experiments, chloride salts were used. In these experiments, Ag/AgCl electrodes were connected to the solution by means of 3 M KCl agar bridges. The membrane was destroyed by tapping on the chamber, and the resulting voltage change was recorded. The liquid junction potential was calculated using the Henderson equation (Lakshminarayanaiah, 1969) and was subtracted from the measured potential.

RESULTS

Rectifying Properties of the Channel

Steady-state currents measured in hemocyanin-treated bilayers are far from being ohmic, and this has been explained as the result of a voltage-dependent distribution of channels in different conductance states (Latorre et al., 1975). The relaxation of this process takes a time on the order of seconds to minutes. If current is measured in a millisecond scale, redistribution of conductance states has no time to occur. In this time scale, the current-voltage relation is not linear either, but it is less nonlinear than the steady-state currents both in single and many-channeled membranes (Alvarez et al., 1975). In Fig. 1, several *I-V* curves for potassium and lithium are shown. In all cases, the current going from the *cis* to the *trans* side is larger than that going in the opposite direction. In most cases, for positive potentials, current increases less than linearly. For negative potentials, however, current can increase less than linearly or more than linearly depending on the concentration of the ion used.

This nonlinearity found at short times can be explained either by a fast voltage-dependent change of the channel structure leading to a change in conductance, or by a fixed structure having nonlinear conductance. To solve this problem, we have measured membrane current during a voltage step with

a resolution in the microsecond range.[1] The result of a typical experiment is shown in Fig. 2. The *top records* in Fig. 2 *A–C* represent the point-by-point difference of the current measured during voltage pulses of ±50, ±100, and ±175 mV, respectively, in a hemocyanin-treated membrane. The shape of the curves arises from the exponential rise and fall of the membrane potential, and the nonlinearity of the current-voltage curves. At ±50 mV, the "on" response is clearly slower than the "off" response, and there is a delay. This can be explained in terms of the shape of the current-voltage relationship (e.g., Fig. 1 *A*), which is symmetric at for $V < 20$ mV. Because of this characteristic of the *I-V* relationship, during the time that the potential is <20 mV, no current difference will be seen and a delay is generated. At the "off" condition, no delay is expected and the current must fall rapidly, *faster than the potential*, because it becomes zero as soon as the voltage drops below 20 mV. We have modeled this hypothesis with a dummy membrane with the same R-C characteristics as the hemocyanin-treated membrane, taking into account both the shape of the current-voltage relationship and the characteristics of the current-to-voltage converter (see the legend to Fig. 2). In the middle of Fig. 2 *A–C* are the current time-courses obtained from the model for ±50, ±100, and ±175 mV, respectively. The bottom part of Fig. 2 shows a superposition of those records at the top and middle of Fig. 2. Inasmuch as the records coincide almost perfectly, the conclusion of Fig. 2 is that, with the time resolution we have, current passing through hemocyanin-treated membranes is a function of potential only, and no time-dependent processes need to be invoked.

This experiment alone does not prove that the structure of the hemocyanin channel does not change with the membrane potential, but we will assume from this point that this is the case. We will therefore try to develop a model to explain the current asymmetry without assuming structural changes using absolute reaction rate theory (Glasstone et al., 1941).

Hemocyanin Channel Selectivity and the Conductance Activity Plane

To begin the formulation of the model, we must know which are the ionic species transported through the channel. Zero current-voltage measurements of hemocyanin-treated membranes separating KCl solutions of different concentrations demonstrate that potassium ions are the main current carriers. Fig. 3 shows a series of zero-current potentials when a hemocyanin-treated membrane separates a 14-mM K_2SO_4 solution from K or Li sulfates at different concentrations. The slope of the linear part of the curve is 55 mV

[1] We have previously reported experiments showing that the current extrapolated at zero time is the same for either positive or negative potentials (Latorre et al., 1975). For positive potentials, we reported a fast relaxation of the channel conductance with a relaxation time on the order of 300 μs. In those early experiments, the capacitative transient current saturated our current-to-voltage converter and the oscilloscope amplifiers for 100 μs. We have not been able to see this relaxation using capacitative transient suppression and digital signal subtraction. We believe that the early results are in error, and that the fast relaxation found was the result of amplifier recovery from saturation.

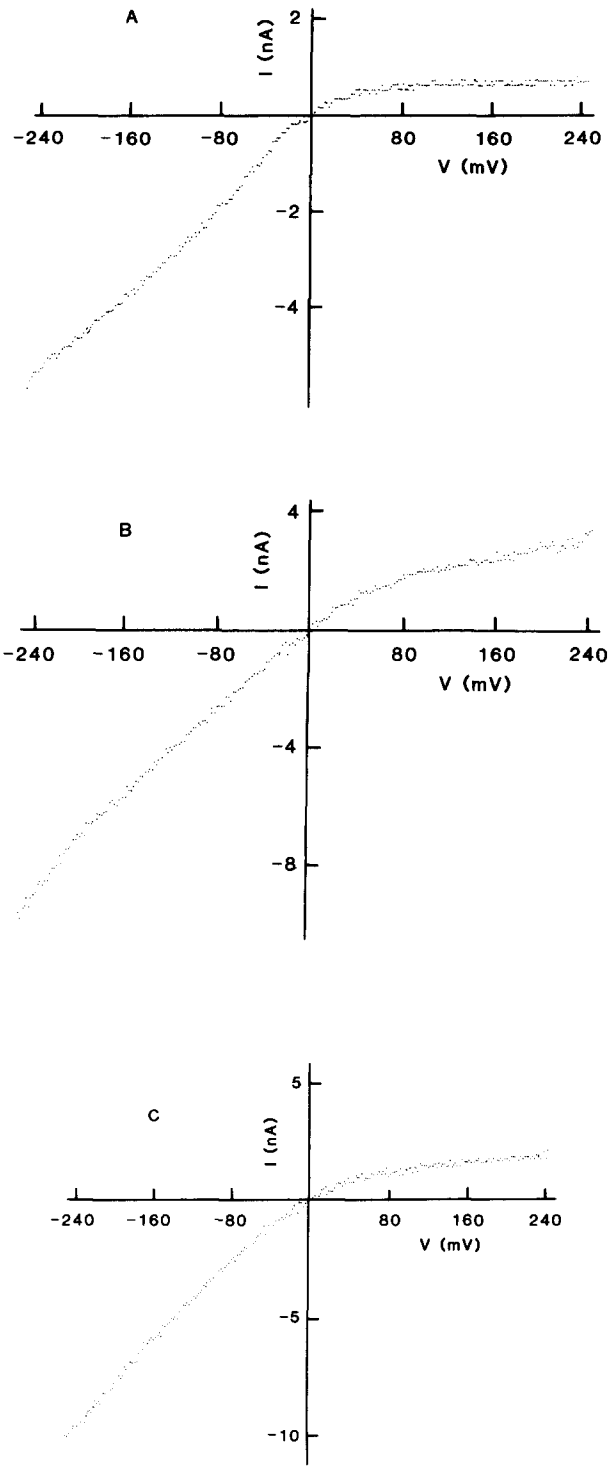

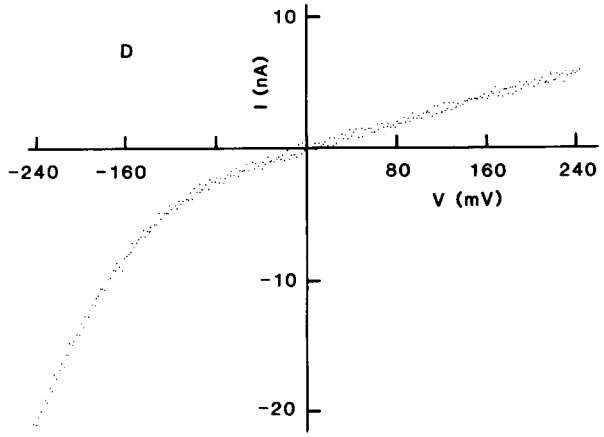

FIGURE 1 (*opposite and above*). Instantaneous current-voltage curves. *A*, 10 mM K_2SO_4; *B*, 500 mM K_2SO_4; *C*, 10 mM Li_2SO_4; *D*, 250 mM Li_2SO_4. Before addition of hemocyanin, the values of the capacitance and series resistance of the R-C network were adjusted to minimize the capacitance current surge at the leading edge of the pulse. Hemocyanin was added to the membrane, and after the conductance increased, the instantaneous *I-V* curves were measured using short pulses of variable amplitudes. Only the current sample is taken after 1 ms of the leading edge of the pulse. Each *I-V* curve is a collection of 250 data points taken from −250 to +250 mV at intervals of 2 mV. A complete *I-V* curve is obtained in only 10 s, insuring that the number of hemocyanin channels is constant.

and the sign of the potential indicates that the current is transported by cations.[2] When KCl is used instead of K_2SO_4, the slope is 50 mV per decade.

The second important point is the dependence of the single-channel conductance, λ_{ch}, on ion concentration. Fig. 4 shows that λ_{ch} is a nonlinear function of the K or Li sulfate salt concentration, which is well represented as a hyperbolic function. Using more soluble KCl, we have measured single-channel conductance up to 2 M potassium activity, and we found that the conductance never decreases as activity is increased. At high salt activities, we found that the channel conductance follows the selectivity sequence K > Rb ≥ NH_4 > Na > Cs > Li. At 500 mM cation activity, the ratio $(\lambda_{ch})_K/(\lambda_{ch})_{Na}$

[2] The transference number of the cation is accordingly 0.97, which indicates that the "mobility" of K^+ in the channel is ~30-fold larger than that of $SO_4^=$. Although this is a trivial correction at low potentials, the $SO_4^=$ mobility may become a problem at large potentials. This is because the applied potential in the Eyring formulation will increase the rate constant for the divalent anion much more than the rate constant for the monovalent cation. To test whether sulphate ions were affecting our interpretation of the magnitudes of the energies given in Table I, we ran a series of experiments with potassium-TES (2 Tris-(hydroxy methyl) methyl amino ethane sulfonic acid). TES is nonovalent and a larger anion than sulphate. Under these conditions, the shape of the instantaneous *I-V* curves was the same as that shown in Fig. 1*A* and *B*. Furthermore, these curves are in good agreement with those obtained theoretically using the parameters of Table I. We conclude that sulfate does not appreciably affect the energy values given in Table I.

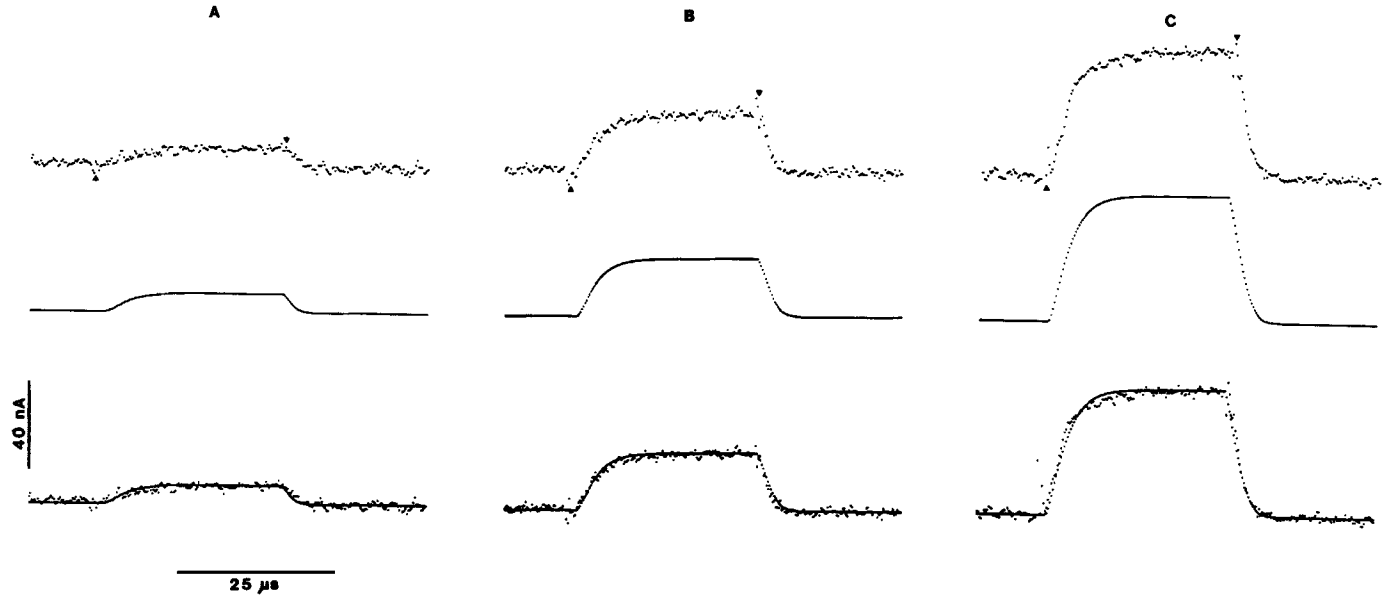

FIGURE 2. "Instantaneous" rectification. The records at the top are the point-by-point difference of the current passing through a hemocyanin-treated membrane during a positive and a negative voltage pulse. Capacitative current was eliminated from the records using a differential ammeter with one input connected to the membrane and the other to an R-C series combination that simulates the transient current. The remainder of the transient was eliminated by the addition of pulses of the same amplitude and opposite polarity. This membrane was formed in 50 mM potassium sulfate with 5 mM Tris-Cl. Membrane capacitance was 490 pF; series resistance was 5,900 ohms. Hemocyanin concentration was 20 μg/ml. *Triangles* mark the "on" and the "off" of the potential pulse. *Curves* at the middle are calculated reading the voltage at each time point from the R-C combination used to compensate for the capacitative surge current. The current responding to each voltage was obtained from the *I-V* relationship of the same membrane. The curve was finally generated by simulating the current amplifier rise time of 1 μs and using the convolution integral. The delay apparent in the ±50 mV curve arises from the fact that current is the same at either polarity if $V < 20$ mV. Since the experimental and computed curves have the same time-course (*bottom records*), we conclude that current is a function of voltage and it is not a function of time. *A*, ±50 mV applied potentials; *B*, ±100 mV applied potentials; *C*, ±175 mV applied potentials.

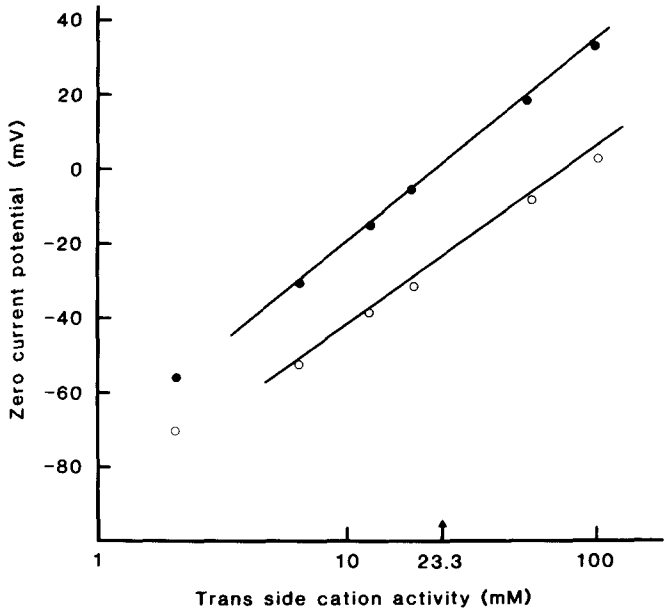

FIGURE 3. Zero-current voltage across hemocyanin-treated bilayers separating asymmetric solutions. The *cis* side contains hemocyanin, 5 mM Tris-Cl buffer, pH 7, and 14 mM K_2SO_4. Potassium activity in the *cis* side is 23.3 mM and it is indicated by the *vertical arrow*. The *trans* side contains 5 mM Tris-Cl buffer, pH 7, and K (*filled circles*) or Li (*open circles*) sulfate. Cation activity in the *trans* side is indicated in the horizontal logarithmic scale. Asolectin membranes were formed under 5 mM Tris-Cl buffer. Hemocyanin and K_2SO_4 were added to the *cis* side and conductance was monitored using 10-mV negative pulses. When conductance increased significantly above the bare bilayer conductance, K or Li sulfate was added to the *trans* side. Both solutions were stirred continuously using magnetic stirring bars. The electrodes were disconnected from the pulse generator and connected to the high-impedance voltmeter. Zero-current potential was recorded, and when a constant value was obtained, the membrane was intentionally broken and the resulting voltage jump was recorded. The voltage after subtracting the calculated liquid junction potential for the boundary left when the membrane was destroyed is presented in this figure. *Solid lines* were calculated using the parameters obtained from the three-barrier model (see text).

= 1.5. A detailed discussion of the selectivity properties of the hemocyanin channel will be a matter for a separate communication.

The hyperbolic function can be explained by a model where only one ion can occupy the channel at a given time (Läuger, 1973; Latorre et al., 1975).[3]

[3] Antolini and Menestrina (1979) and Menestrina and Antolini (1981) have given a different interpretation to the channel conductance vs. activity curves. They suggested that channel conductance saturation arises as a consequence of negative charges located on the inner wall of the channel. We think that this possibility is unlikely inasmuch as we do not find that the conductance tends to reach a lower limit at low ionic activities as expected of a wide pore with fixed negative charge (e.g., Latorre et al. [1972]).

Channel conductance in this model is proportional to the ion concentration, C, and the probability that the channel is available (1-f):

$$\lambda_{ch} = KC(1\text{-}f) \tag{1}$$

where K is the probability of an ion entering into an empty channel per unit time and unit salt activity. Channel conductance is also proportional to the probability of finding an occupied channel and inversely proportional to the mean transit, T. Thus,

$$\lambda_{ch} = \frac{Af}{T} \tag{2}$$

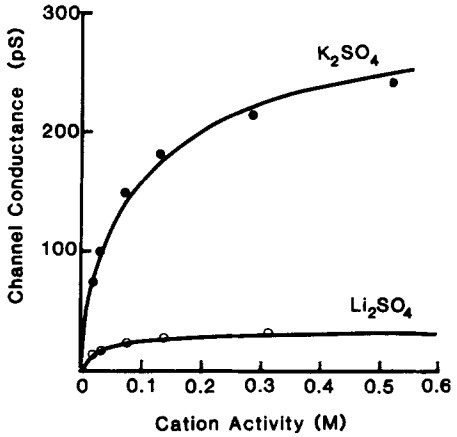

FIGURE 4. Single-channel conductance; sulfate salts, asolectin membranes. *Solid lines* were calculated from the model. Membranes were formed under solutions of various compositions and concentrations as indicated by the absissa. Hemocyanin was added to the *cis* side, and the *trans* side was polarized to −50 mV. Current was recorded continuously, and it increased stepwise every time a hemocyanin channel was incorporated into the bilayer. The average amplitude of the conductance jumps is plotted on the ordinate. The average was taken from 10 to 100 individual conductance jumps; standard deviation was always <10% of the average.

where A is a constant of proportionality. Combining Eqs. 1 and 2 we obtain

$$\lambda_{ch} = \frac{AC/T}{A/KT + C}. \tag{3}$$

Eq. 3 predicts channel conductance saturation in the conductance-activity plane. However, this model cannot account for the shape of the I-V curves shown in Fig. 1. If the maximum conductance of the channel is assumed to be voltage independent, I-V curves calculated from the model would always be sublinear, the rate of entrance to the channel being the rate-limiting step at

high voltages. To explain the superlinear *I-V* curves observed at high concentrations, the transient time of ions must be a function of voltage. We will explain these features by modeling the entrance of an ion into the channel and the transport within the channel as jumps over energy barriers.

Measurements of the current as a function of voltage at low potassium concentrations show that current becomes voltage independent at >80 mV, as seen in Fig. 1.[4] This result can be explained by assuming that the entry of potassium into the channel from the *trans* side is a jump over a *voltage-independent* energy barrier, a barrier located external to the electric field.[5] For negative potentials, the shape of the *I-V* curves is more complicated; from 0 to −50 mV, the slope of the *I-V* curve increases with potential, but at >80 mV, the slope of the curve decreases. In the interval from 0 to −50 mV, the rate-limiting step appears to be a jump over an energy barrier that decreases when voltage increases, a barrier located in the field. This superlinear part of the *I-V* curve is better seen at 500 mM K_2SO_4 at voltages > −200 mV (Fig. 1 *B*) and in lithium *I-V* curves (Fig. 1 *C* and *D*).

The Three-Barrier Model

The inspection of the *I-V* curves suggests a model in which there are two energy barriers located external to the field that represent the rate of ion entry into the channel from the *cis* and *trans* sides, and are apparent in the *I-V* curves as saturating or sublinear regions. A third energy barrier represents the rate of transport of ions inside the channel; it varies with the applied potential and is apparent in the *I-V* curves as superlinear portions. These three barriers define two energy wells representing two binding sites located at the *cis* and *trans* mouths of the channel. To be consistent with the one-ion-per-channel assumption postulated above, ions can only be at one binding site at a given time.

We will develop a set of equations to solve for the steady-state ion current using the Eyring absolute reaction rate theory (Glasstone et al., 1941). The first step in the formulation of the model is to define the three possible states of the channel: state 0: no ions in the channel; state 1: one ion at the *cis* binding site; and state 2: one ion in the *trans* binding site. Six rate constants represent the rate of transition connecting the three states as defined in Fig. 5.

Rate constants k_1 and k_{-3} involve the binding of one ion from the solution to the channel and are functions of ion concentration. The magnitude of each rate constant depends on an energy term that is the difference of energy

[4] At very large potentials (>200 mV), current increases sharply in some membranes, which suggests the breakdown of the membrane structure. This breakdown is more notorious if Tris is not present in the solutions. We used Tris buffer in all the experiments to have a simpler experimental situation.

[5] Saturation of the current in the first quadrant can also be explained if we assume that the exit of potassium from the channel is the rate-limiting step. If the condition of single-ion occupancy is imposed on this model, the current in the first quadrant should be independent of the ion concentration at high potentials, since the channel would be occupied all the time. This prediction contradicts the experimental observations as shown below.

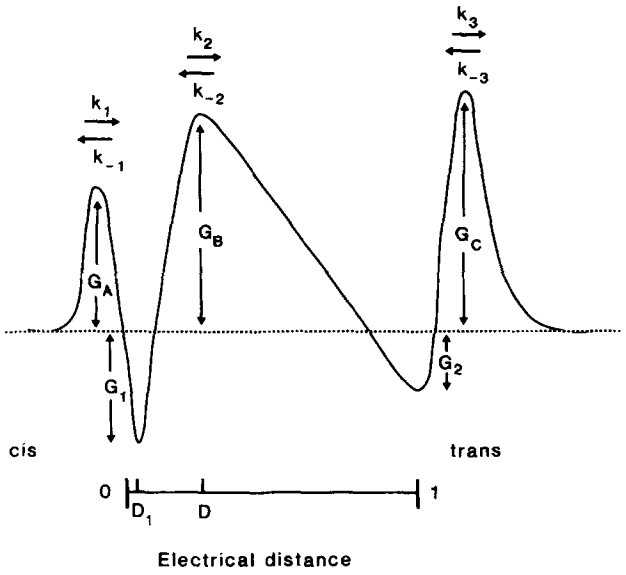

FIGURE 5. The three-barrier model. In this figure, k_i is the rate constant of the ion movement through three energy barriers from the *cis* to the *trans* side. k_i is the rate constant for jumps from the *trans* to the *cis* side. Kinetic rate constants are functions of the energy jump involved in each transition. The energy in the *cis* side is taken as the reference state and is defined as zero. The energy in the *trans* side is changed by the applied electric potential. The boundaries drawn represent the region of the channel where the voltage drops; the distances D_1 and D are measured in units of fraction of the total voltage drop. G_1 and G_2 are the energy minima at each of the binding sites. The two lateral barriers, with energies G_A and G_C, are related to the rate of entrance of ions from the bulk solutions into the channel from the *cis* and *trans* sides, respectively. G_B is the height of the energy barrier related to the transport of ions within the channel.

between the initial state and the height of the barrier separating it from the final state, because only one ion is allowed in each energy well.

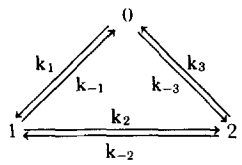

Fig. 5 shows a graphic representation of the peaks and wells. The contribution of the applied electric potential to the rate constants is explicitly introduced into the model, assuming that the central peak is located at a fraction D down the electric field from the *cis* mouth of the channel. The potential need not be assumed to drop linearly along the channel and therefore the D's need not correspond exactly to linear distances (Hille, 1975).[6] Accord-

[6] To fit the data, an additional distance, D_1, representing the position of well 1 is needed. The distance of well 2 need not be taken different from unity.

ingly, the rate constants are given by the following expressions:

$$k_1 = C\exp(-G_A)$$
$$k_{-1} = \exp[(G_1 + D_1U) - G_A]$$
$$k_2 = \exp[(G_1 + D_1U) - (G_B + DU)]$$
$$k_{-2} = \exp[(G_2 + U) - (G_B + DU)]$$
$$k_3 = \exp(G_2 - G_C)$$
$$k_{-3} = C\exp(-G_C)$$
$$C \equiv \text{bulk ion concentration}$$
$$U \equiv eV/kT$$

In steady state, the probabilities *P0*, *P1*, and *P2* of finding the channel in each of the three states can be calculated using the graphic method of King and Altman (Segel, 1975) and the expressions found are:

$$P0 = k_{-1}k_{-2} + k_3(k_2 + k_{-1})$$
$$P1 = k_{-3}k_{-2} + k_1(k_{-2} + k_3)$$
$$P2 = k_{-3}k_{-1} + k_2(k_1 + k_{-3}).$$

The steady-state ion current is the net transition rate across any energy barrier:

$$I = Q(P0 \times k_1 - P1 \times k_{-1})/(P0 + P1 + P2).$$

In this equation, $Q = 10^6$ pA/channel, assuming that the frequency factor is unity. The denominator arises from the necessary condition that all three probabilities must add up to one. Given a set of values for the energy peaks and wells, and the distances D and D_1, this paradigm of equations allows us to compute the ionic current as a function of ion concentration and voltage. We estimate these seven parameters using an iterative least-square nonlinear regression curve-fitting program (Table I). The results of the curve-fitting for the *I-V* curves taken for potassium concentrations ranging from 20 to 1,000 mM show that the energy minima and the central peak change consistently with salt concentration, and the other parameters do not change. Energy wells are deeper and the central peak is lower at low concentrations than at high concentrations. These changes are in the same direction of the changes in membrane surface potential as a function of salt concentration.[7] To examine more closely the effect of surface potential on these energy values, we use the average values of the entrance energy barrier and the electrical distances as fixed parameters to compute new values for the energy wells and the central

[7] When a bilayer is made with a mixture of asolectin and cholesterol, negatively charged groups are expected to be on the membrane surface with a density of one every 500 Å^2. The electrostatic surface potential decreases when salt concentration decreases because surface charge is shielded by counter-ions. The surface potential is calculated using the equation that relates surface charge density and surface potential for mixed electrolytes (Aveyard and Haydon, 1973).

energy barrier. With the straight lines describing the change of the parameters G_1, G_2, and G_B, the potassium current can now be calculated as a function of concentration and potential. These new values are plotted on Fig. 6 in which the contribution of surface potential on these parameters is clearly seen. The energy minima, G_1 and G_2, change more than the central barrier, G_B.

The results of these calculations are computed with the experimental points in Fig. 7 and the fit is quite good. The *solid curves* drawn in Fig. 4 are also computed for the model. From these two figures we can conclude that the three-barrier model can explain well the experimental data in the conductance-activity plane and in the current-voltage plane for potassium and lithium in negatively charged asolectin membranes.

Tests of the Three-Barrier Model

Using this model and the parameters already defined, we can predict several new characteristics of hemocyanin channels. For example, we can predict the shape of the *I-V* curves for noncharged membranes treated with hemocyanin by reading the appropriate parameters from the *straight lines* in Fig. 6. Our model predicts that for a membrane with no surface charge the wells will be

TABLE I

PARAMETERS FOR THE THREE-BARRIER MODEL

Membrane	Ion	Concentration	G_1	G_2	G_A	G_B	G_C	D	D_1
Asolectin	K	50 mM	−3.41±0.06	−1.35±0.04	5.16±0.34	7.86±0.05	8.36±0.12	0.265±0.008	0.042±0.005
Asolectin	Li	50 mM	−4.17±0.03	−1.56±0.11	6.10±0.12	9.57±0.04	9.18±0.16	0.362±0.020	0.066±0.009

Parameters can be calculated for any concentration if the contribution of the surface potential is taken into account as shown in Fig. 6. Energies are given in units of kT. G_A, G_C, D, and D_1 are the terms of the parameters calculated at different concentrations. G_1, G_2, and G_B are estimated from the regression lines of Fig. 5. Dispersion measurements are standard errors.

less deep than in charged membranes at any ion concentration. In addition, in noncharged membranes, the central energy barrier will be higher. Experimental *I-V* curves for asolectin and phosphatidylethanolamine (PE) membranes are compared in Fig. 8. The current passing through the hemocyanin channels is larger in PE than in asolectin at the same concentration, and the *I-V* curve for PE is superlinear in the third quadrant. Both experimental findings are consistent with the model. The current is larger because the wells are less deep in PE membranes, making the exit of ions from the channel faster than in asolectin. The *I-V* curves are superlinear because the ion transport becomes the rate-limiting step since the central barrier is higher. The solid line drawn over the experimental points in the PE curve of Fig. 8 was calculated from the model using the parameters found for asolectin for the outer energy peaks, G_A and G_C, and the positions of the wells and central peak, D and D_1. The energies of the two wells and the central peak are those found for zero surface charge from Fig. 6. Since the fit is reasonable using the parameters for asolectin membranes, we think that this is a good test for the proposed effect of surface potential on the parameters of the model.

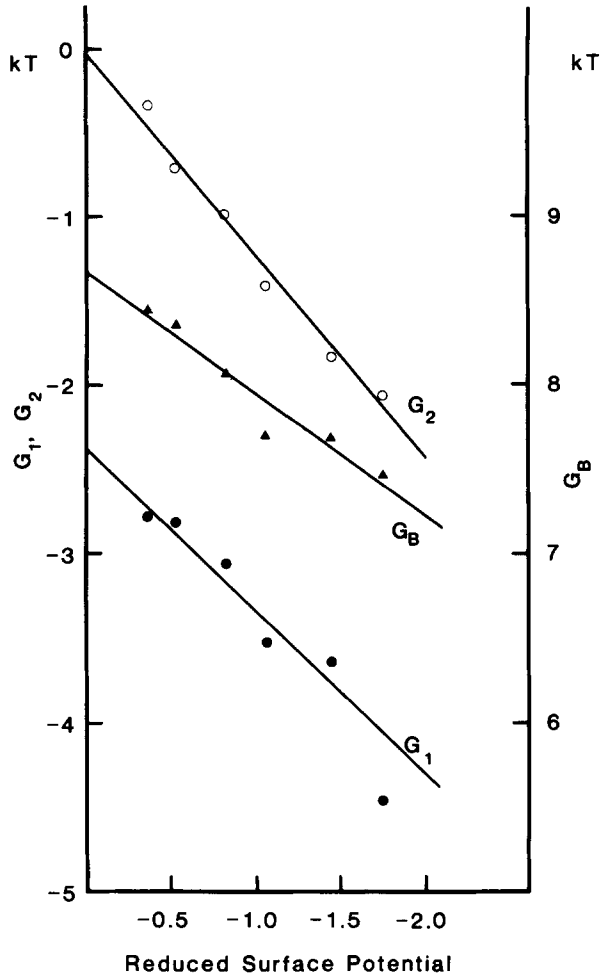

FIGURE 6. Effect of surface charge on G_1, G_2, and G_B. This is the result of the curve-fitting of the potassium *I-V* curves, leaving G_1, G_2, and G_B as the only adjustable parameters. The values of the parameters in kT units are plotted as a function of the reduced surface potential. Reduced surface potential = $e\phi_s/kT$, where ϕ_s is the surface potential. ϕ_s was calculated assuming a surface density of one negative charge for every 500 Å^2. The *solid lines* are described by the following equations: $G_1 = -2.41 \pm 0.12 - 0.95 \pm 0.14|\psi_s|$; $G_2 = -0.06 \pm 0.10 - 1.24 \pm 0.09|\psi_s|$; $G_B = 8.63 \pm 0.11 - 0.73 \pm 0.10|\psi_s|$, where ψ_s is the reduced surface potential. For lithium, the equations are: $G_1 = -2.66 \pm 0.07 - 1.44 \pm 0.06|\psi_s|$; $G_2 = -0.07 \pm 0.36 - 1.42 \pm 0.25|\psi_s|$; $G_B = 10.80 \pm 0.12 - 1.17 \pm 0.10|\psi_s|$. The parameters of the straight lines were obtained using five points for Li and six points for K.

Another prediction of the model is the magnitude of the single-channel conductance in the presence of mixtures of potassium and lithium. According to the model, single-channel conductance in the presence of lithium will be different from the conductance measured for potassium alone. There are three

reasons for this change. First, lithium flow will contribute to the total current; this effect increases conductance. Second, channels occupied by lithium will not be available for potassium; since single-channel lithium conductance is smaller than for potassium, this effect will decrease single-channel conductance. Finally, the addition of lithium will decrease the surface potential; this effect will increase conductance because the energy wells, G_1 and G_2, will be

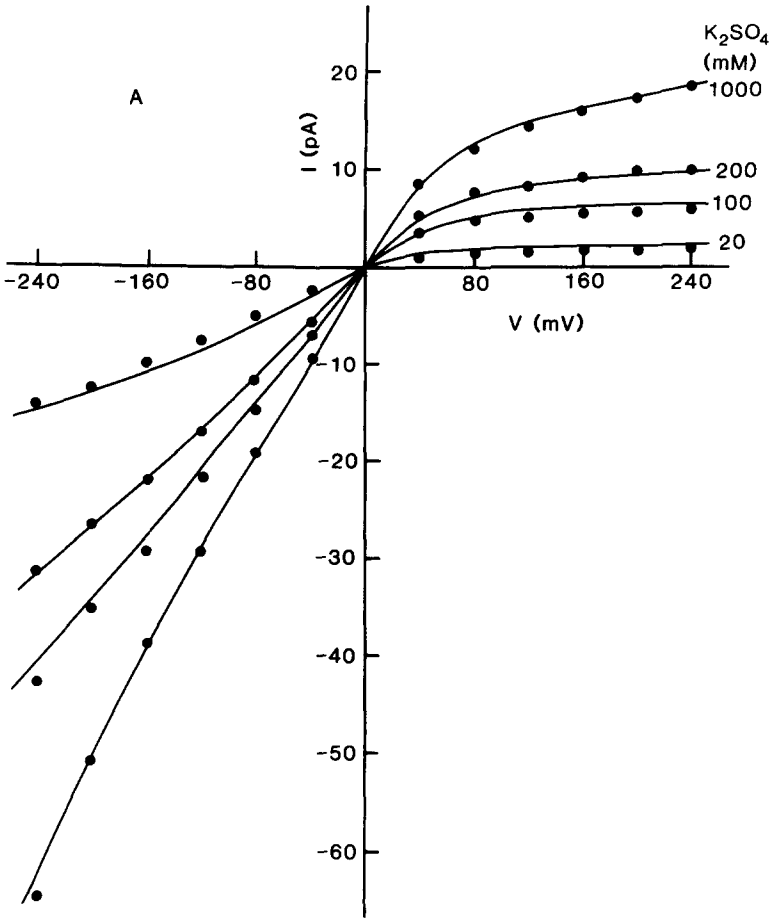

FIGURE 7. Theoretical *I-V* curves. *Solid lines* are calculated using the parameters determined from the straight lines in Fig. 6. *A*, potassium; *B*, lithium.

less deep as seen when hemocyanin-treated asolectin and PE membranes are compared. The final balance of these three effects can be evaluated using the three-barrier model. To calculate the current, the model must be extended to allow five different states of the channel: O: channel empty; 1K: channel with K ion in well 1; 2K: one K ion in well 2; 1Li: one Li ion in well 1; 2Li: one Li ion in well 2. The probabilities of finding each of these five states can be

calculated by considering, first, the states involving K and the states involving Li independently (Segel, 1975). In a second step, the probabilities are combined to give the final probabilities; e.g., the probability of having one K ion in well 1 is the probability of having a K ion in the well in the absence of lithium times the probability of having a channel without lithium if there was no potassium. Fig. 9 shows the results of these calculations for various combinations of K and Li, together with the experimentally measured single-channel conductance. We feel that the agreement of theory and experiment

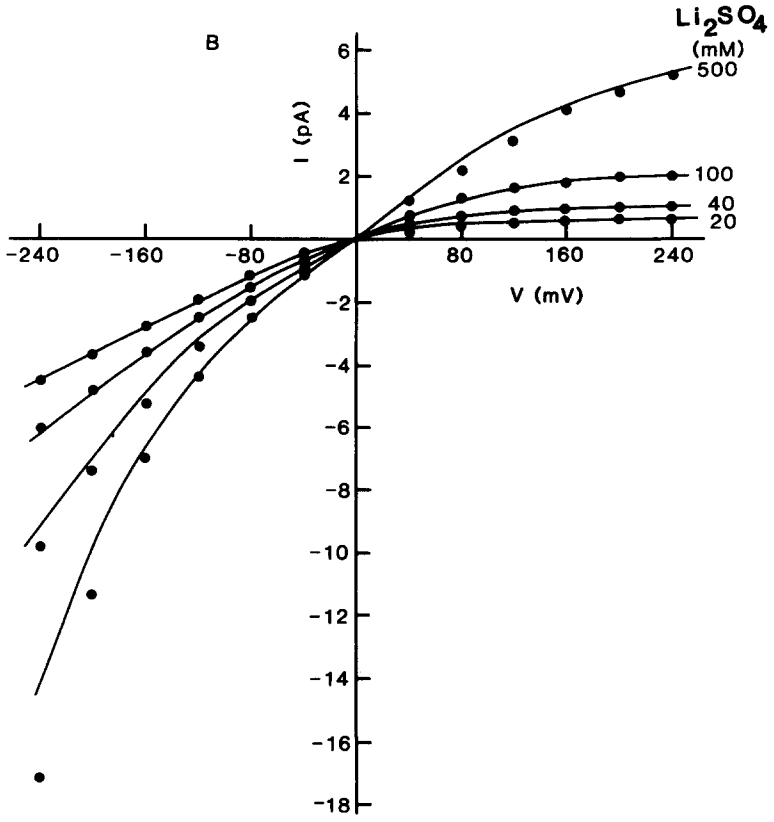

FIGURE 7B.

is reasonably good considering the number of assumptions made and given the fact that there are no adjustable parameters involved in the calculations.

A third experimental result predicted by the model is the zero-current voltage recorded when a hemocyanin-treated membrane separates asymmetric solutions. The problem is solved by evaluating the current passing through the channel at various values of voltage and interpolating the voltage for $I = 0$ using the parameters of the model. The comparison of the theoretical curves and experimental data is presented in Fig. 3 for asymmetric solutions and for

K in the *cis* side and Li in the *trans* side. The fit is reasonably good because no adjustable parameters are involved in the calculation.

We feel that the three-barrier model developed for the hemocyanin channel is a good model because not only can it describe well the initial observations used to formulate it, but it can also predict successfully new phenomena such as *I-V* curves in neutral membranes, lithium-potassium competition, and zero-current potentials for asymmetric solutions.

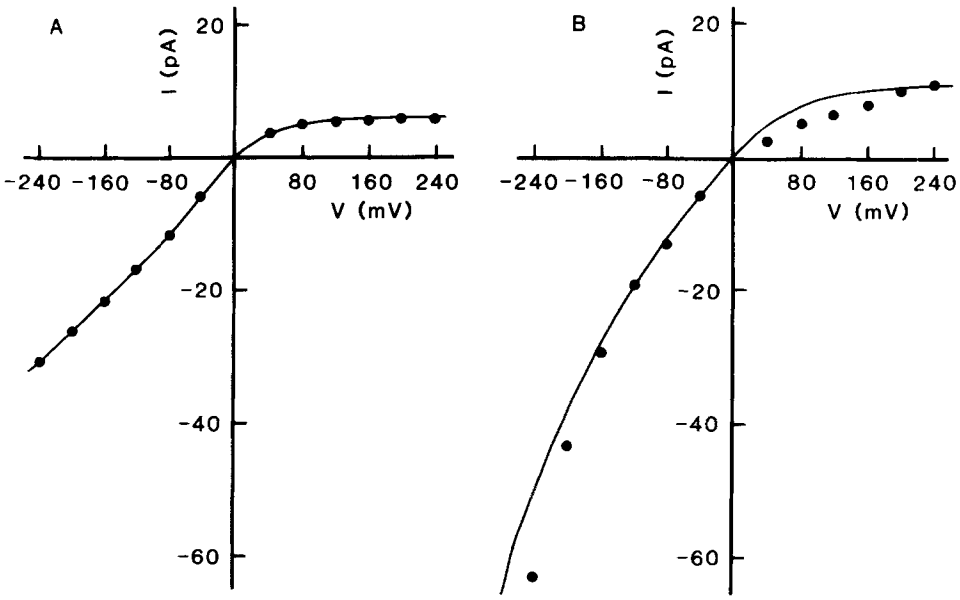

FIGURE 8. Effect of surface charge on *I-V* curves. *A*, *I-V* curve for potassium current through hemocyanin-treated asolectin membrane (negative surface). The *solid line* is the *I-V* curve computed using the parameters indicated in Table I. *B*, *I-V* curve obtained in a phosphatidylethanolamine membrane (neutral surface). The *solid line* was computed using the parameters G_A, G_C, D, and D_1 listed in Table I for asolectin membranes. Parameters G_1, G_2, and G_B are those found for zero surface potential from Fig. 6. Currents were scaled down as described in Methods. Aqueous phases were 50 mM K_2SO_4, 5 mM Tris-Cl, pH 7.0.

DISCUSSION

In general, open channels cannot be viewed as structures filled with an electrolyte solution in which ion movement is governed by free diffusion. Examples of processes not explained by the electrodiffusion theory are flux coupling, flux saturation, and other phenomena that have been the subject of several reviews (e.g., Armstrong [1975 *a* and *b*]; French and Adelman [1976]). In nerve, most of the properties of the open sodium channel are accounted for by a four-barrier, three-site model. This model also assumes

that only one ion is allowed inside the channel at a time (Hille, 1975). The potassium channel presents the additional difficulty of ions moving in single file (Hodgkin and Keynes, 1955) and is better represented by a multi-barrier, multi-ion model (Hille and Schwarz, 1978). Even the results obtained in channels that present large conductance and poor selectivity cannot be explained by the traditional electrodiffusion picture of ions moving independently of each other. This is the case of the acetylcholine-activated channel

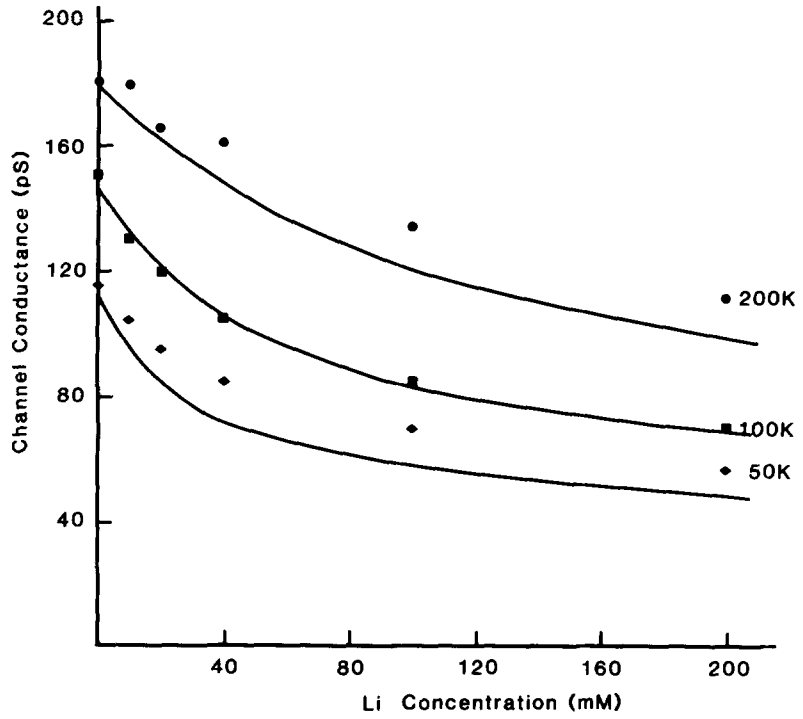

FIGURE 9. Lithium-potassium competition. Single-channel conductance was measured at −50 mV in the presence of both K and Li. We used three different K concentrations: 50, 100, and 200 mM. Solutions were prepared at these concentrations containing various concentrations of lithium as indicated in the *horizontal axis* of the figure. *Dots* are the experimental points and *lines* are the result of the calculations of single-channel current using the three-barrier model.

found in the neuromuscular junctions. For this type of channel, a two-barrier, single-site model is able to account for the experimental results (Lewis and Stevens, 1979). All the barrier models referred to above are based on the absolute reaction rate theory (Glasstone et al., 1941). In lipid bilayer membranes, on the other hand, ion transport through the gramicidin A channel has been extensively studied (Hladky and Haydon, 1972; Läuger, 1973; Sandblom et al., 1977; Levitt, 1978; Hladky et al., 1979; Andersen and

Procopio, 1980). Although there is no general agreement with respect to what potential energy profile best describes the experimental results (cf. Levitt [1978]; Sandblom et al. [1977]), it is clear that water must move in single file (Rosenberg and Finkelstein, 1978; Levitt et al., 1978). Furthermore, as pointed out by Anderson and Procopio (1980), models trying to describe the ion movement through the gramicidin A channel probably will need to account explicitly for movement of water through the channel.

In the present paper, we have developed an energy barrier model that generates the shape of the instantaneous *I-V* relations, single-channel conductance saturation, inhibition, and open circuit potentials, which we measure in hemocyanin channels. The picture of the hemocyanin channel given by this model does not call for structural changes of the channel to account for the nonlinear instantaneous *I-V* curves. The ion transport mechanism is different from simple electrodiffusion in two aspects: first, only one ion is allowed into the channel at a time, and there is one main energy barrier that must be overcome by the ion moving into the channel.

Effect of Surface Potential

The surface potential produced by ionizable head groups of the phospholipids forming a bilayer has been extensively studied by using ion carriers as probes (for review see McLaughlin [1977]). All the results of the carrier studies demonstrate that the membrane conductance changes with surface potential as predicted by changes in surface ion concentration as expected from a Boltzmann distribution, the surface potential being well described by the diffuse double-layer theory of Gouy. In other words, if cations are the current carriers, conductance will be enhanced in negatively charged membranes. In agreement with this expectation, gramicidin single-channel conductance is higher at low electrolyte concentrations in negatively charged membranes than in neutral membranes (Apell et al., 1979). On the other hand, we have found that although hemocyanin is a protein inducing a cation conductance, single-channel conductance is smaller (>80 mV) in membranes bearing negative charge, as compared with neutral membranes. This paradox is explained in terms of the three-barrier model proposed here for the hemocyanin channel. The effect of surface charge on the hemocyanin channel is to decrease the potential energy (G_1 and G_2) of ions in the binding sites, whereas the heights of the energy barriers for the exit of ions from the channel to the surrounding solutions (G_A and G_C) is not affected by surface potential. The rate constant of ion exit is smaller in charged membranes because it depends on the energy difference between the binding site and the peak of exit barrier. Ion transport through the central peak is not greatly affected by changes in surface charge density because the height of the central barrier and the depth of the two wells vary to roughly the same extent.

Conductance in the hemocyanin channel near zero voltage represents the rate of ion transport inside the channel. Conductance at high voltage, on the other hand, is dominated by the rate of entry or exit of ions to and from the channel. This explains why the conductance difference between charged and

neutral membranes is seen only at high voltages and is not seen near zero voltage. The simplest effect of surface potential would be to change all the energy values for peaks and wells to the same extent (constant field assumption and all peaks and wells inside the membrane). To our surprise, we found that the energy peaks for the entry and exit of ions (G_A and G_C) do not vary with changes in surface potential. This lack of effect of surface potential changes can be explained if these barriers are located outside of the diffuse double layer potential (see Fig. 10). There are structural bases for believing that this is the case for the hemocyanin channel. McIntosh et al. (1980) have reported that keyhole limpet hemocyanin is able to form structures that project from the membrane surface into the aqueous phase by 2.5–4.5 nm. They also report that these structures present a central pool of stain of 2 nm in diameter. The Debye length for a 1,2 electrolyte at 10 mM (the lowest concentration used in this work) is 1.8 nm. If we locate the mouth of the channel at 2.5 nm away from the surface of the bilayer, this point will "feel" only 25% of the double layer potential. This is an upper limit because in the above calculation we used the minimum value for ion strength and the shortest projection for the molecule into the aqueous phase, as reported by McIntosh et al. (1980). The independence of the outer energy barriers, G_A and G_C, with surface potential can be easily explained by locating these peaks near the mouth of the channel.

The result that the central energy barrier, G_B, is less (~20%) sensitive to changes in surface potential as compared with the two energy wells, G_1 and G_2, may have several explanations, the most straightforward being that the charge density in the channel is not zero. This charge can be given by ionizable groups or dipoles in the hemocyanin molecule. This leads to an attenuation of the potential with the distance from the membrane surface. It could also be the result of systematic errors in the estimation of the energy parameters caused by other changes occurring in the channel that are not included in our three-barrier model.

Physical Interpretation of the Three-Barrier Model

Fig. 10 is a pictorial representation of a hemocyanin channel in a negatively charged lipid bilayer membrane. The double-layer potential is represented at the top of the figure and it has been drawn keeping in mind that the solution bathing the membrane is 25 mM K_2SO_4 (Debye length, ~1.4 nm). The hemocyanin channel has been drawn in such a way that it projects 4 nm away from the membrane surface to be consistent with the structures seen under the electron microscope (McIntosh et al., 1980). In this pictorial representation, the entrance and exit of the channel feels only a small fraction of the double layer potential.

Fig. 10 also shows that when ions cross the outer barrier, they go from a potential level equal to the bulk solution to an energy level that is dependent on surface membrane potential. This represents, therefore, the transfer of ions from the bulk solution to a binding site located near the plane described by the membrane surface. The rate-limiting step of this transfer must be a jump over an energy barrier located at the entrance of the channel, >1 Debye

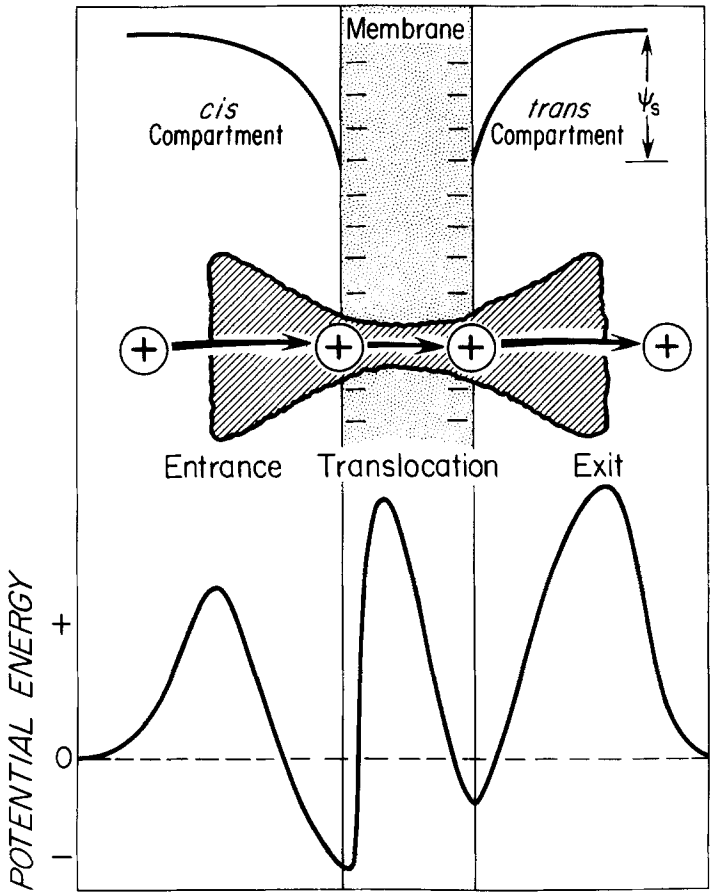

FIGURE 10. Schematic representation of a model for ion translocation through the hemocyanin channel. *Top*: the negatively charged lipids contained in soybean lipids produce a negative electrostatic potential in the aqueous phase immediately adjacent to the membrane. In the bulk aqueous phase this potential is zero. The potential profile in the figure is that predicted by the Gouy-Chapman theory for a 25 mM K_2SO_4 solution (Debye length, ~1.4 nm). *Middle*: the protein forming the channel is shown. It projects 4 nm away from the membrane surface at each side to be consistent with the picture of the channel obtained by McIntosh et al. (1980) using the electron microscope. In this way, both the entrance into and exit from the channel are located >1 Debye length away from the membrane surface. *Bottom*: the lower part represents the energy profile of the potassium ion in the channel when no voltage is applied across the membrane. The peaks over the zero line represent energy barriers and the valleys under it represent binding sites for the ion in the channel. All distances drawn for peaks and valleys are arbitrary.

length away from the membrane surface. The positions of all peaks and valleys in the distance coordinates are arbitrary. They have just been located to show that the external peaks do not feel the surface potential, whereas the binding sites and the central peak do. We have arbitrarily shaped the structure

of the channel as an hourglass. The smaller diameter of the channel-forming protein at the membrane surface allows for the surface potential changes to be reflected in the center of the structure (Apell et al., 1979).[6]

The fact of having found a simple barrier model to account for all the experimental observations is an important step in the further study of ion transport mechanisms through the hemocyanin channel. Furthermore, we think that the hemocyanin channel can be a useful model for the inward rectification found in many biological preparations such as that observed in vertebrate skeletal muscle (Adrian and Freygang, 1962), heart muscle membrane (Noble and Tsien, 1968), and echinoderm egg (Hagiwara and Takahashi, 1974).

We thank Drs. D. Benos and R. French for critical reading of the manuscript and the referees of this paper for very helpful remarks. We also thank Mr. Juan Espinoza for his able technical assistance and for the construction of our digital computer and data acquisition system. We are grateful to Marianita Sanchez whose patience goes beyond her secretarial duties.
This work was supported by the University of Chile grant B-250-781 and by the National Institutes of Health grant GM-25277.

Received for publication 23 September 1980 and in revised form 24 July 1981.

REFERENCES

ADRIAN, R. H., and W. H. FREYGANG. 1962. The potassium and chloride conductance of frog muscle membrane. *J. Physiol. (Lond.)*. **163**:61–103.

ALVAREZ, O., and R. LATORRE. 1978. Voltage-dependent capacitance in lipid bilayer membranes made from monolayers. *Biophys. J.* **21**:1–17.

ALVAREZ, O., E. DIAZ, and R. LATORRE. 1975. Voltage-dependent conductance induced by hemocyanin in black lipid films. *Biochim. Biophys. Acta.* **389**:444–448.

ALVAREZ, O., J. REYES, and R. LATORRE. 1977. Ion transport through the hemocyanin channel. *Biophys J.* **17**:214*a*. (Abstr.).

ANDERSEN, O. S., and J. PROCOPIO. 1980. Ion movements through gramicidin A channels. On the importance of the aqueous diffusion resistance and ion-water interactions. *Acta Physiol. Scand. Suppl.* **481**:27–35.

ANTOLINI, R., and G. MENESTRINA. 1979. Ion conductivity of the open keyhole limpet hemocyanin channel. *FEBS Lett.* **100**:377–381.

APELL, H. J., E. BAMBERG, and P. LAUGER. 1979. Effects of surface charge on the conductance of the gramicidin channel. *Biochim. Biophys. Acta.* **552**:369–378.

ARMSTRONG, C. M. 1975 *a*. K pores of nerve and muscle membranes. *In* Membranes, a Series of Advances. G. Eisenman, editor. Marcel Dekker, Inc., New York. **3**:325–358.

ARMSTRONG, C. M. 1975 *b*. Ionic pores, gates and gating currents. *Q. Rev. Biophys.* **7**:179–210.

AVEYARD, R., and D. A. HAYDON. 1973. An introduction to the principles of surface chemistry. Cambridge University Press, London. 200 pp.

EHRENSTEIN, G., and H. LECAR. 1972. The mechanism of signal transmission in nerve axons. *Annu. Rev. Biophys. Bioeng.* **1**:347–368.

FERNANDEZ-MORAN, H., E. F. J. VAN BRUGGEN, and M. OHTSUKI. 1966. Macromolecular organization of hemocyanins and apohemocyanins as revealed by electron microscopy. *J. Mol. Biol.* **16**:191–207.

FRENCH, R. J., and W. J. ADELMAN, JR. 1976. Competition, saturation, and inhibition—ionic

interactions shown by membrane ionic currents in nerve, muscle, and bilayer systems. *Curr. Top. Membr. Transp.* **8**:161–207.

GLASSTONE, S., K. J. LAIDLER, and H. EYRING. 1941. The theory of rate processes. McGraw-Hill Book Company, New York. 355 pp.

HAGIWARA, S., and K. TAKAHASHI. 1974. The anomalous rectification and cation selectivity of the membrane of a starfish egg cell. *J. Membr. Biol.* **18**:61–80.

HILLE, B. 1970. Ionic channels in nerve membranes. *Prog. Biophys. Mol. Biol.* **21**:1–32.

HILLE, B. 1975. Ionic selectivity, saturation and block in sodium channels. A four-barrier model. *J. Gen. Physiol.* **66**:535–560.

HILLE, B., and W. SCHWARZ. 1978. Potassium channels as multiion single-file pores. *J. Gen. Physiol.* **72**:409–442.

HLADKY, S. B., and D. A. HAYDON. 1972. Ion transfer across lipid bilayers in the presence of gramicidin A. *Biochim. Biophys. Acta.* **274**:294–312.

HLADKY, S. B., B. W. URBAN, and D. A. HAYDON. 1979. Ion movements in pores formed by gramicidin A. *In* Membrane Transport Processes. C. F. Stevens and R. W. Tsien, editors. Raven Press, New York. **3**:89–103.

HODGKIN, A. L., and R. D. KEYNES. 1955. The potassium permeability of a giant nerve fibre. *J. Physiol. (Lond.)*. **128**:61–88.

LAKSHMINARAYANAIAH, N. 1969. Transport phenomena in membranes. Academic Press, Inc., New York. 517 pp.

LATORRE, R., O. ALVAREZ, G. EHRENSTEIN, M. ESPINOZA, and J. REYES. 1975. The nature of the voltage-dependent conductance of the hemocyanin channel. *J. Membr. Biol.* **25**:163–181.

LATORRE, R., G. EHRENSTEIN, and H. LECAR. 1972. Ion transport through excitability-inducing material (EIM) channels in lipid bilayer membranes. *J. Gen. Physiol.* **60**:72–85.

LAUGER, P. 1973. Ion transport through pores. A rate theory analysis. *Biochim. Biophys. Acta.* **311**:423–441.

LEVITT, D. G. 1978. Electrostatic calculations for an ion channel. II. Kinetic behavior of the gramicidin A channel. *Biophys. J.* **22**:221–248.

LEVITT, D. G., S. R. ELIAS, and J. M. HARTMAN. 1978. Number of water molecules coupled to the transport of Na^+, K^+, and H^+ via gramicidin, nonactin, and valinomycin. *Biochim. Biophys. Acta.* **512**:436–451.

LEWIS, C. A., and C. F. STEVENS. 1979. Mechanism of ion permeation through channels in a postsynaptic membrane. *In* Membrane Transport Processes. C. F. Stevens and R. W. Tsien, editors. Raven Press, New York. **3**:133–151.

MCINTOSH, T. J., J. D. ROBERTSON, H. P. TING-BEALL, A. WALTER, and G. ZAMPIGHI. 1980. On the structure of the hemocyanin channel in lipid bilayers. *Biochim. Biophys. Acta.* **601**:289–301.

MCLAUGHLIN, S. 1977. Electrostatic potentials at membrane-solution interfaces. *In* Current Topics in Membrane and Transport. F. Bonner and A. Kleinzeller, editors. Academic Press, Inc., New York. **9**:71–145.

MELLEMA, J. E., and A. KLUG. 1972. Quaternary structure of gastropod hemocyanin. *Nature (Lond.)*. **239**:146–150.

MENESTRINA, G., and R. ANTOLINI. 1981. Ion transport through hemocyanin channels in oxidized cholesterol artificial bilayer membranes. *Biochim. Biophys. Acta.* **643**:616–625.

MONTAL, M., and P. MUELLER. 1972. Formation of bimolecular membranes from lipid monolayers and a study of their electrical properties. *Proc. Natl. Acad. Sci. U. S. A.* **67**:1265–1275.

NOBLE, D., and W. TSIEN. 1968. The kinetics and rectifier properties of the slow potassium current in cardiac Purkinge fibers. *J. Physiol. (Lond.)*. **195**:185–214.

PARLIN, R. B., and H. EYRING. 1954. Membrane permeability and electrical potential. *In* Ion Transport Across Membranes. H. T. Clarke, editor. Academic Press, Inc., New York. 103–118.

ROSENBERG, P. A., and A. FINKELSTEIN. 1978. Interaction of ions and water in gramicidin A channels: streaming potentials across lipid bilayer membranes. *J. Gen. Physiol.* **72**:327–340.

SANDBLOM, J., G. EISENMAN, and E. NEHER. 1977. Ionic selectivity, saturation and block in gramicidin A channels. I. Theory for the electrical properties of ion selective channels having two pairs of sites and multiple conductance states. *J. Membr. Biol.* **31**:383–417.

SEGEL, I. M. 1975. Enzyme Kinetics. John Wiley & Sons, Inc., New York. 506–517.

VAN BRUGGEN, E. F. J., V. SCHUITEN, E. H. WIEBENGA, and M. GRUBER. 1963. Structure and properties of hemocyanins from different gastropoda and crustacea. *J. Mol. Biol.* **7**:249–253.

VAN BRUGGEN, E. F. J., E. H. WIEBENGA, and M. GRUBER. 1962 *a*. Structure and properties of hemocyanins. I. Electron micrographs of hemocyanin and apohemocyanin from *Helix pomatia* of different pH values. *J. Mol. Biol.* **4**:1–7.

VAN BRUGGEN, E. F. J., E. H. WIEBENGA, and M. GRUBER. 1962 *b*. Structure and properties of hemocyanins. II. Electron micrographs of the hemocyanins of *Sepia officinalis*, *Octopus vulgaris*, and *Cancer pagurus*. *J. Mol. Biol.* **4**:8–9

WOODBURY, J. W. 1971. Eyring rate theory and model of the current-voltage relationship of ion channels in excitable membranes. *In* Chemical Dynamics: Papers in Honor of Henry Eyring. J. Hirschfelder, editor. John Wiley & Sons, Inc., New York. 601–617.